Electronic supplementary information

Spin unlocking oxygen evolution reaction on antiperovskite nitrides

Huang Tang[a, ‡], Deshuai Yang[b, ‡], Mengfei Lu[a,c, ‡], Shaoxi Kong[a], Yanghui Hou[a], Duanduan Liu[a,c], Depei Liu[a,c], Shicheng Yan[a,*], Zhaoxu Chen[b,*], Tao Yu[c] and Zhigang Zou[a,c]

[a] Jiangsu Key Laboratory of Artificial Functional Materials, Eco-materials and Renewable Energy Research Center (ERERC), Collaborative Innovation Center of Advanced Microstructures, College of Engineering and Applied Sciences, Nanjing University, Nanjing, Jiangsu 210093, P. R. China, E-mail: yscfei@nju.edu.cn

[b] School of Chemistry and Chemical Engineering, Nanjing University, Nanjing, Jiangsu 210093, P. R. China, E-mail: zxchen@nju.edu.cn

[c] Jiangsu Key Laboratory for Nano Technology, National Laboratory of Solid State Microstructures, School of Physics, Nanjing University, Nanjing, Jiangsu 210093, P. R. China

Supplementary Text

Calculations of e_g filling. The temperature-dependent magnetizations (M) for the $Cu_{0.5}NFe_{3.5}$ and $Cu_{0.5}NFe_3Ni_{0.5}$ under H = 1 kOe were shown in Fig. 2a. Above 700 K, the magnetic susceptibility (χ= M/H) calculated from the magnetization intensity obeyed to the paramagnetic Curie-Weiss law: χ= C/(T-θ), where C is the Curie constant and θ is the Curie-Weiss temperature (Fig. 2b). The Curie constant C could be calculated and the effective magnetic moment $\mu_{eff} = \sqrt{8C}\mu_B$ of all samples could be obtained. The final calculated values were plotted in Fig. 2c. The effective magnetic moment was calculated without considering the contribution of Cu^{2+}, by using the formula of $\mu_{eff}^2 = \mu_{Fe}^2 + \mu_{Ni}^2$. Since Ni^{2+} has only a unique spin state ($3d^8$ $e_g^2 t_{2g}^6$), the effective magnetic moment of Ni^{2+} was: $\mu_{Ni} = g\mu_B\sqrt{S(S+1)}$, where G = 2, G is the Lande factor, and S (= 1) is the spin quantum number of Ni^{2+}. Thus, the effective magnetic moment μ_{Fe} of Fe^{3+} could be obtained. Then, according to the relation: $\mu_{Fe} = g\mu_B\sqrt{S_{HS}(S_{HS}+1)V_{HS} + S_{LS}(S_{LS}+1)V_{LS}}$, the volume fraction of Fe^{3+} in high spin (HS) and low spin (LS) states could be calculated, where S_{HS} (= 5/2) and S_{LS} (= 1/2) were the spin quantum number of the high spin state and the low spin state, respectively, and the spin quantum number is half of the number of all unpaired electrons in the spin state, and V_{HS} and V_{LS} (= 1-V_{HS}) were the volume fraction of Fe^{3+} under HS and LS, respectively. Consequently, the e_g electron (x) could be further calculated by x = S'$_{HS}$ × V$_{HS}$ + S'$_{LS}$ × V$_{LS}$ = 2 V$_{HS}$. Here S'$_{HS}$ and S'$_{LS}$ were the number of Fe^{3+} e_g electrons under HS and LS, respectively. The calculated results of the e_g electron (x) of Fe^{3+} of $Cu_{0.5}NFe_{3.5}$ and $Cu_{0.5}NFe_3Ni_{0.5}$ were 0.74 and 1.19,respectively.
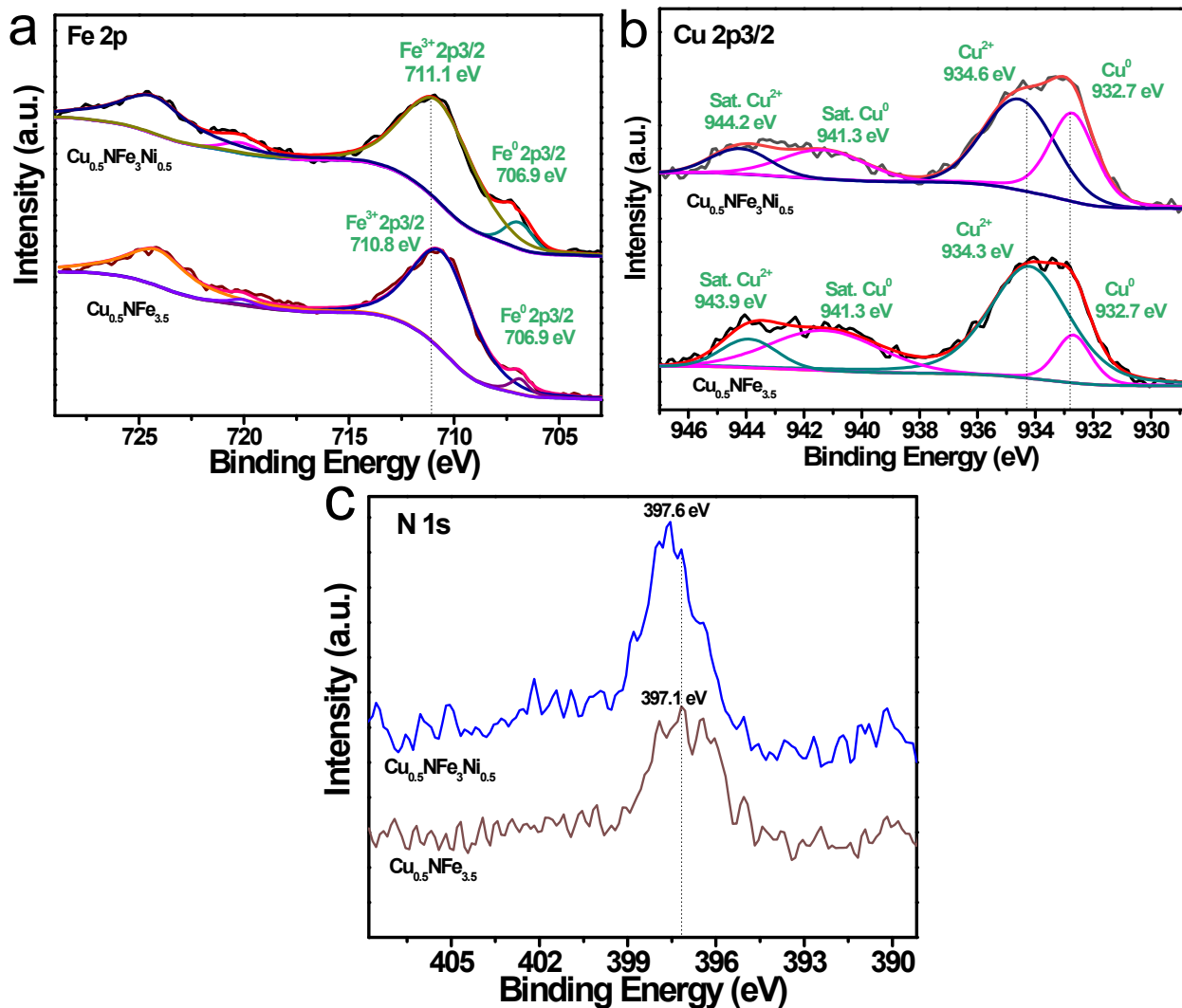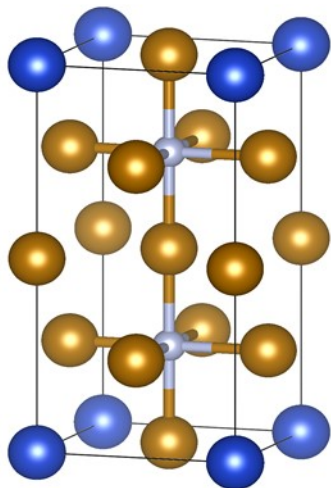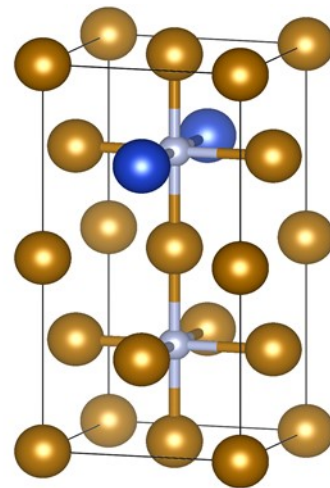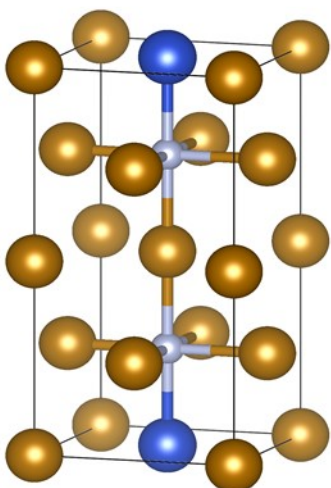
Fig. S1 Effects of Ni doping on XPS spectra of $Cu_{0.5}NFe_{3.5}$. (*a*) Fe 2p. (*b*) Cu 2p3/2. (*c*) N 1s.

Cu at vertex
E= -80.08 eV

Cu at face center 1
E= -78.04 eV

Cu at face center 2
E= -78.01 eV

● Cu

● Fe

○ N

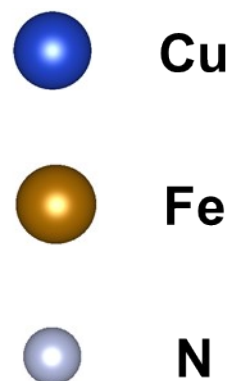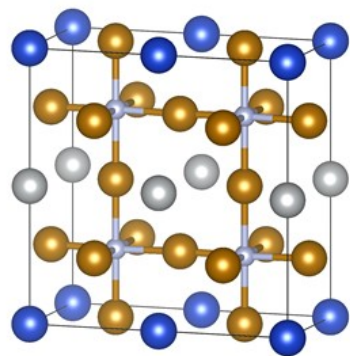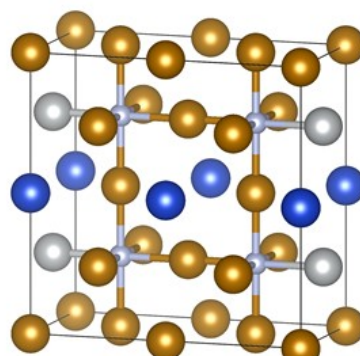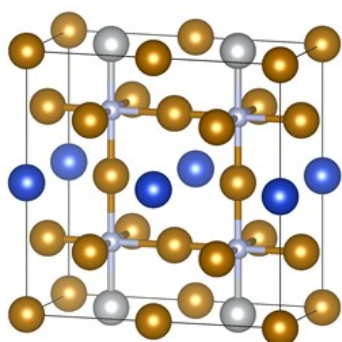**Fig. S2** Optimized structure of $Cu_{0.5}NFe_{3.5}$. Cu at the vertex or at face center. The theoretical calculations indicated that the Cu atoms tend to occupy the vertex of cube.

Fig. S3 Optimized structure of $Cu_{0.5}NFe_3Ni_{0.5}$. Ni at the vertex or at face center. The theoretical calculations indicated that the Ni atoms tend to occupy the vertex of cube.

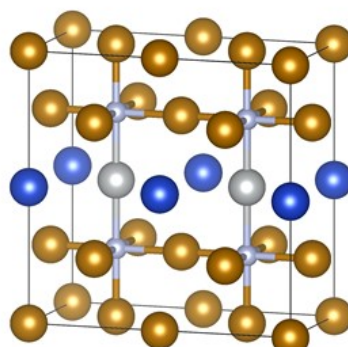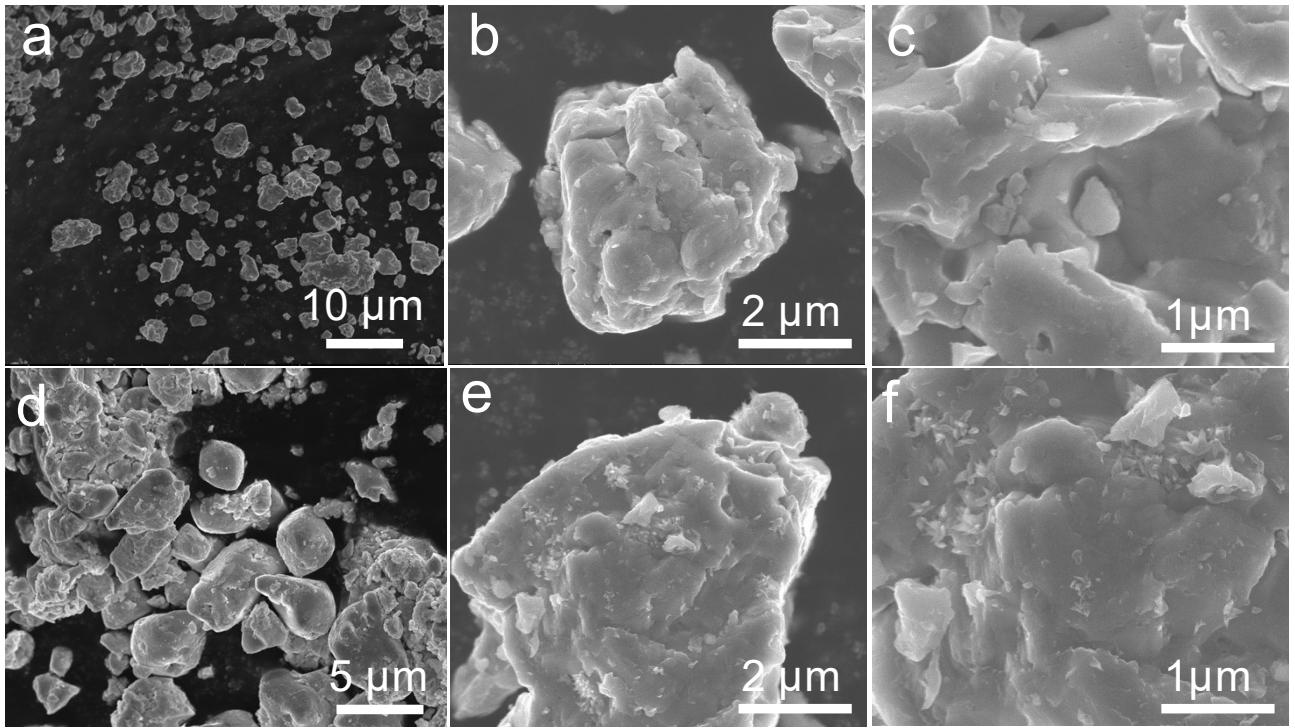**Fig. S4** SEM images. (*a-c*) $Cu_{0.5}NFe_{3.5}$. (*d-f*) $Cu_{0.5}NFe_3Ni_{0.5}$.

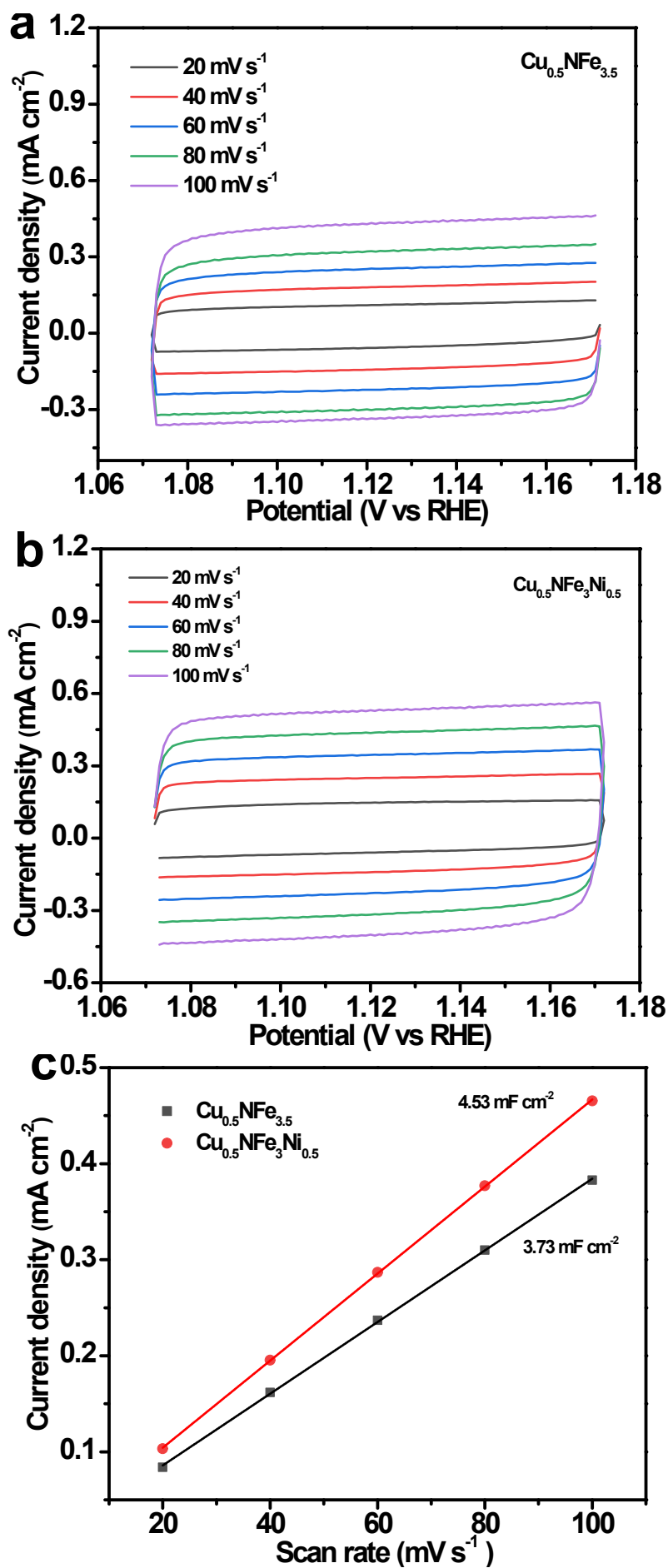**Fig. S5** ECSA measurement. (a) $Cu_{0.5}NFe_{3.5}$. (b) $Cu_{0.5}NFe_3Ni_{0.5}$. (c) The corresponding linear fitting of the capacitive currents versus CV scans.
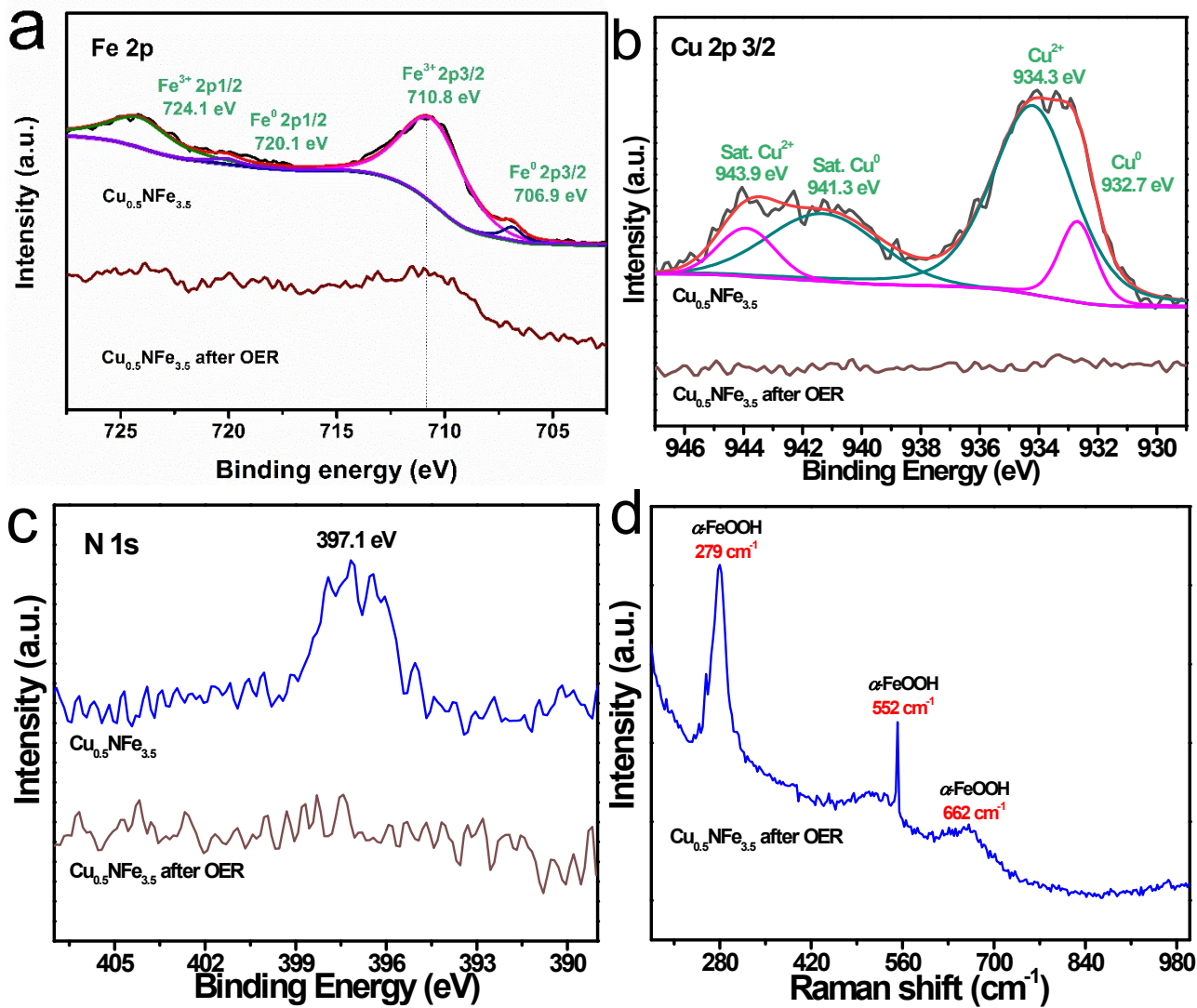
Fig. S6 Changes of surface properties for $Cu_{0.5}NFe_{3.5}$ during OER. (a-c) XPS spectra for Fe 2p, Cu 2p 3/2, and Ni 1s. (d) Raman spectrum.
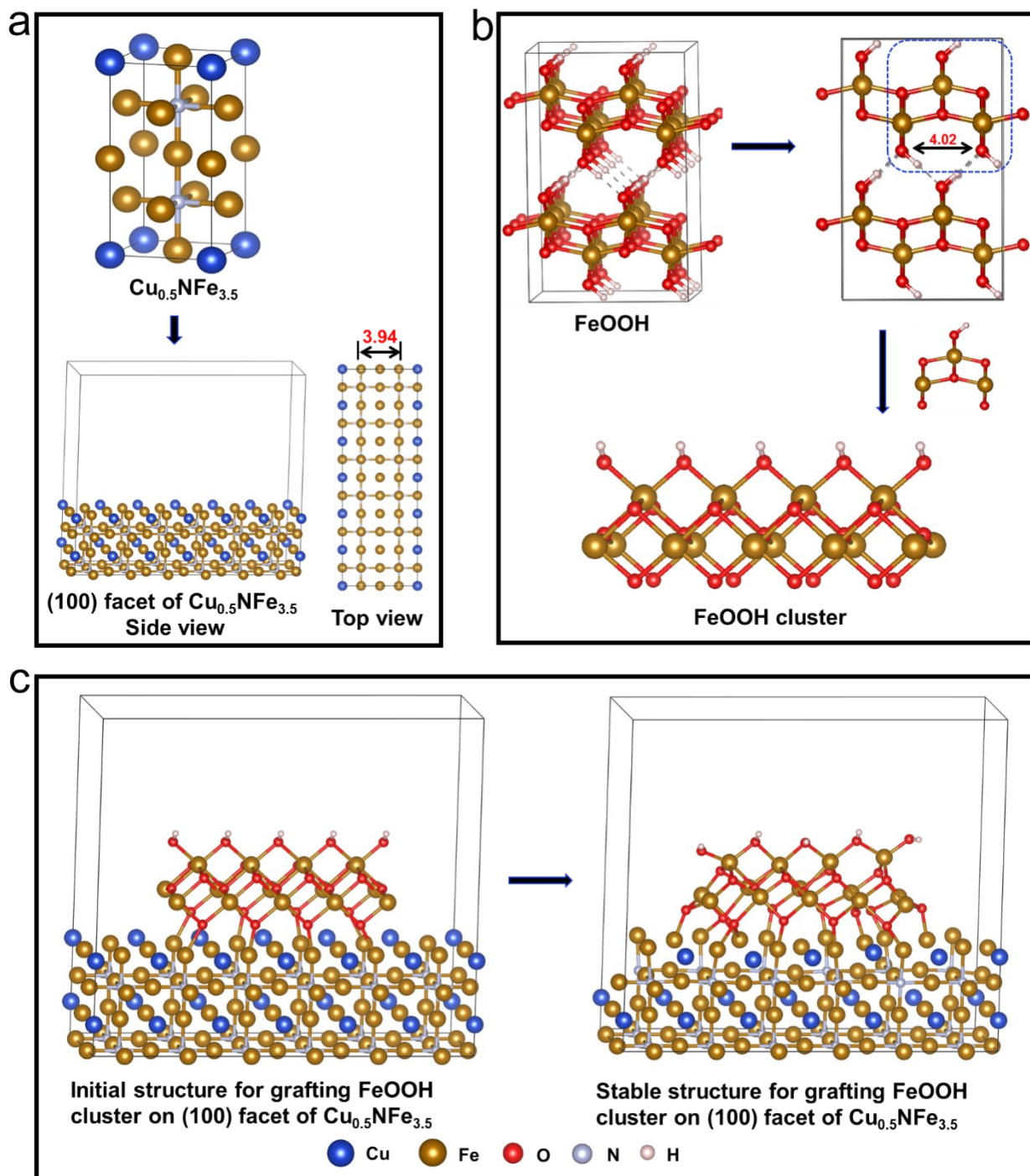
Fig. S7 The structure of grafting FeOOH cluster on (100) facet of $Cu_{0.5}NFe_{3.5}$. (a) The structure of $Cu_{0.5}NFe_{3.5}$ and (100) facet of $Cu_{0.5}NFe_{3.5}$. (b)The structures of FeOOH and its cluster. The FeOOH cluster is constructed by matching the distance between adjacent O atoms of FeOOH and the distance of two Fe atoms on (100) facet of $Cu_{0.5}NFe_{3.5}$. (c) Grafting the FeOOH cluster onto (100) facet of $Cu_{0.5}NFe_{3.5}$.
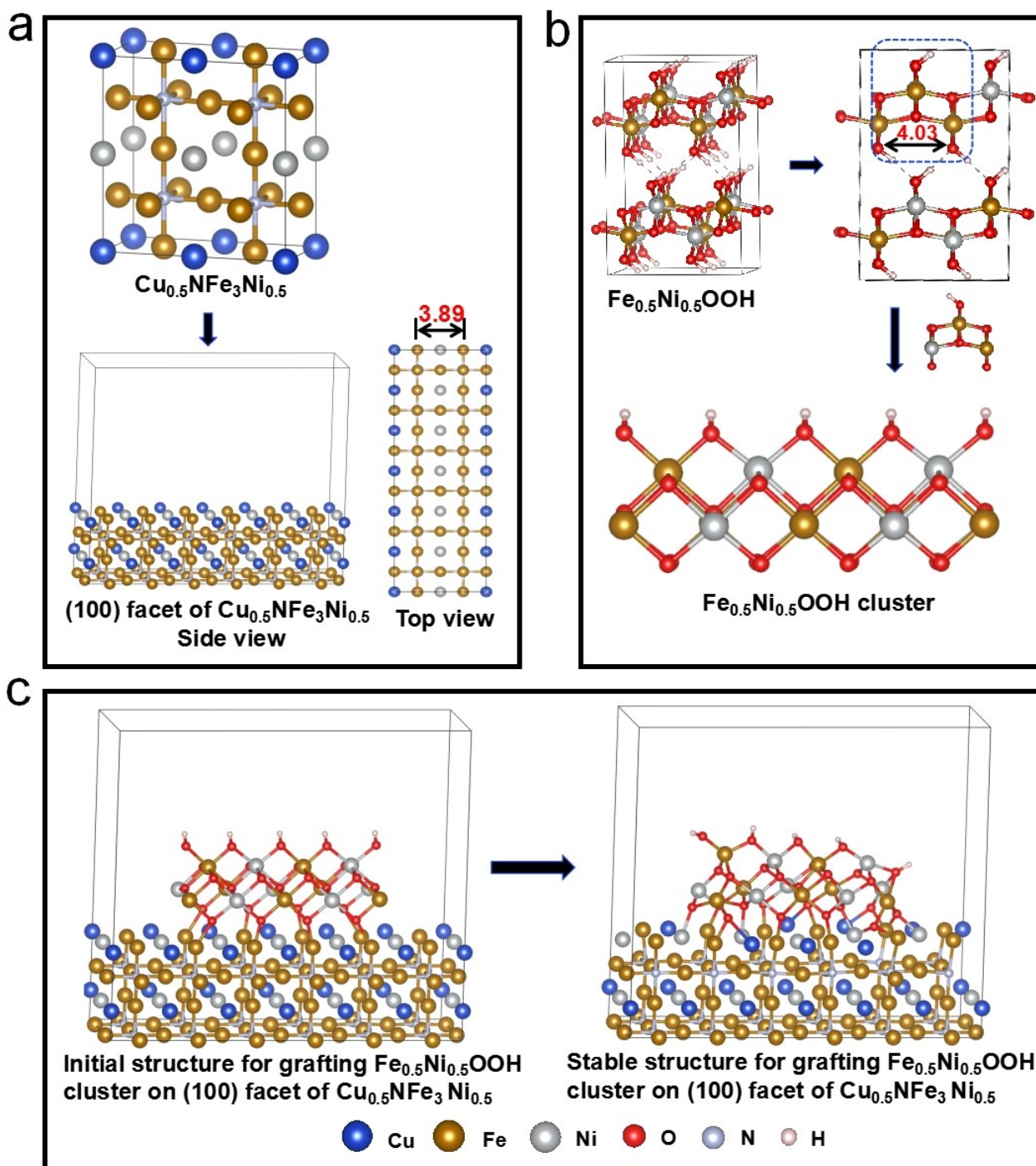
Fig. S8 The structure of grafting $Fe_{0.5}Ni_{0.5}OOH$ cluster on (100) facet of $Cu_{0.5}NFe_3Ni_{0.5}$. (a) The structure of $Cu_{0.5}NFe_3Ni_{0.5}$ and (100) facet of $Cu_{0.5}NFe_3Ni_{0.5}$. (b) The structures of $Fe_{0.5}Ni_{0.5}OOH$ and its cluster. The $Fe_{0.5}Ni_{0.5}OOH$ cluster is constructed by matching the distance between adjacent O atoms of $Fe_{0.5}Ni_{0.5}OOH$ and the distance of two Fe atoms on (100) facet of $Cu_{0.5}NFe_3Ni_{0.5}$. (c) Grafting the $Fe_{0.5}Ni_{0.5}OOH$ cluster onto (100) facet of $Cu_{0.5}NFe_3Ni_{0.5}$.
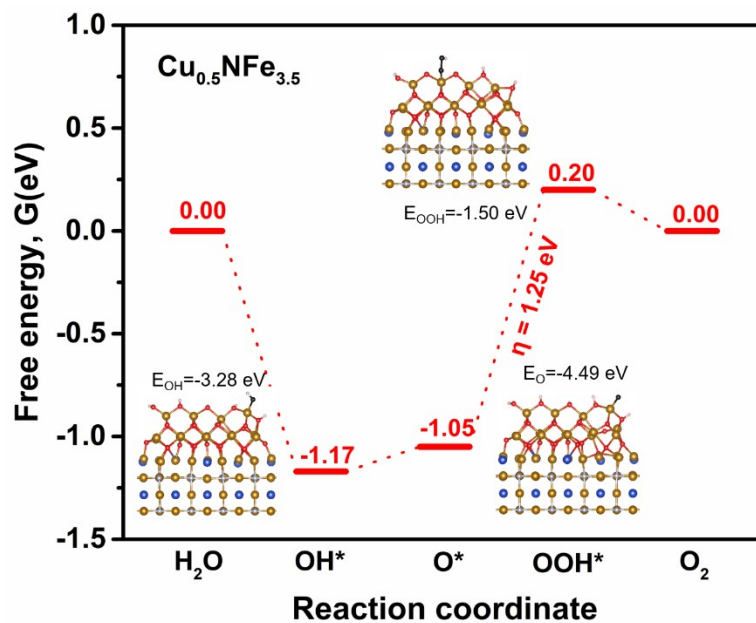
Fig. S9 The free energy diagrams for OER intermediates adsorbing onto paramagnetic FeOOH/paramagnetic $Cu_{0.5}NFe_{3.5}$ at 1.23 V, with calculated structures, adsorbed energy (E) and rate-determining step.

Table S1. Compositions of the samples determined by ICP-OES.

Samples	The content of metal ions (μmol)			Mole ratio	
	Cu	Fe	Ni	Fe/Cu	Fe/Ni
$Cu_{0.5}NFe_{3.5}$	40.76	285.19	/	7.02	/
$Cu_{0.5}NFe_3Ni_{0.5}$	37.40	213.30	35.56	5.7	5.99

Table S2. The comparison of the OER performance of $Cu_{0.5}NFe_3Ni_{0.5}$ with the electrocatalysts currently reported.

Catalyst	Overpotential η (mV)			Tafel slope (mV dec^{-1})	Substrate	Reference
	10 mA cm^{-2}	100 mA cm^{-2}	200 mA cm^{-2}			
$Cu_{0.5}NFe_3Ni_{0.5}$	244	310	340	59	carbon paper (CP)	This work
p-$Cu_{1-x}NNi_{3-y}$/FeNiCu	280	403	-	52	glass carbon (GC)	[1]
$CuNCo_{2.4}V_{0.6}$	235	306	320	52	CP	[2]
Co_4N/CNW	310	510	-	81	carbon cloth (CC)	[3]
Fe_3O_4/Ni_3FeN	290	353	-	43	rotation disk electrode (RDE)	[4]
$InNCo_{2.7}Mn_{0.3}$	300	380	395	84	GC	[5]

Table S3. Fitting parameters of EIS plot shown in Fig.3c by using the Randle's equivalent circuit.

Samples	CPE		C_{ct} (mF)	R_{ct} (ohm)	R_s (ohm)
	n	Q ($\mu\Omega^{-1}$ s^n)			
$Cu_{0.5}NFe_3Ni_{0.5}$	0.99	1672.8	1.59	3.56	6.982
$Cu_{0.5}NFe_{3.5}$	0.94	1818.9	1.49	26.7	7.129
IrO_2	0.72	1204.7	0.28	19.57	5.227

From CPE parameters (Q and n values, Q is the pre-factor of the CPE and n is exponent of the CPE), the capacitance was calculated using equation of $C_{ct}= Q^{1/n}(1/R_s+1/R_{ct})^{(n-1)/n}$ (**Ref.** B. Hirschorn, M. E. Orazem, B. Tribollet, V. Vivier, I. Frateur, M. Musiani, *Electrochim. Acta* 2010, **55**, 6218).

Table S4. The free energy for $Cu_{0.5}NFe_3Ni_{0.5}$ or $Cu_{0.5}NFe_{3.5}$ respectively grafting by $Fe_{0.5}Ni_{0.5}OOH$ or FeOOH cluster with different magnetic ground states.

Samples	ΔE (eV)		
	Ferromagnetic	Ferrimagentic	Paramagnetic
$Cu_{0.5}NFe_{3.0}Ni_{0.5}@Fe_{0.5}Ni_{0.5}OOH$	-936.63727	-937.61613	-938.80571
$Cu_{0.5}NFe_{3.5}@FeOOH$	-1010.0083	-1008.695	-1009.155

Supplementary References

1   Y. Zhu, G. Chen, Y. Zhong, Y. Chen, N. Ma, W. Zhou and Z. Shao, *Nat. Commun.*, 2018, **9**, 2326.

2   J. Zhang, X. Zhao, L. Du, Y. Li, L. Zhang, S. Liao, J. B. Goodenough and M. Cui, *Nano Lett.*, 2019, **19**, 7457-7463.

3   Meng, F., Zhong, H., Bao, D., Yan, J. and Zhang, X. *J. Am. Chem. Soc.*, 2016, **138**, 10226-10231.

4   N. Ma, G. Chen, Y. Zhu, H. Sun, J. Dai, H. Chu, R. Ran, W. Zhou, R. Cai and Z. Shao, *Small*, 2020, **16**, 2002089.

5   L. Du, M. Lv, J. Zhang, H. Song, D. Dang, Q. Liu, Z. Cui and S. Liao, *ACS Appl. Energy Mater.*, 2020, **3**, 5293-5300.